

NLO QCD corrections to $WW+\text{jet}$ production at hadron colliders

Stefan Kallweit¹

in collaboration with S. Dittmaier¹ and P. Uwer²
based on *Phys. Rev. Lett.* **100**, 062003 (2008)

¹Max-Planck-Institut für Physik (Werner-Heisenberg-Institut), München

²Institut für Theoretische Teilchenphysik, Universität Karlsruhe

May 8, 2008, PSI particle theory seminar



Max-Planck-Institut für Physik
(Werner-Heisenberg-Institut)

- 1 Introduction
- 2 Calculation of NLO QCD corrections
 - Virtual corrections
 - Real corrections
 - Collinear subtraction counterterm
- 3 Numerical results & comparison with other groups
- 4 Implementation of W decays
- 5 Preliminary results
- 6 Conclusions & Outlook

Motivation

Why is $pp/p\bar{p} \rightarrow WW + \text{jet} + X$ interesting ?

- **Important background process** at the LHC (and for Tevatron Higgs searches)
“Les Houches experimenter’s wishlist ’05” for important missing NLO predictions:

process

$pp \rightarrow WW + \text{jet}$

Dittmaier/S.K./Uwer '07, Campbell/Ellis/Zanderighi '07

Binoth/Guillet/Karg/Kauer/Sanguinetti (in progress)

$pp \rightarrow t\bar{t}b\bar{b}$

$pp \rightarrow t\bar{t} + 2\text{jets}$

$pp \rightarrow VVb\bar{b}$

$pp \rightarrow VV + 2\text{jets}$

$pp \rightarrow V + 3\text{jets}$

$pp \rightarrow VVV$

background for

$H + \text{jet}, t\bar{t}H, \text{new physics (leptons} + \cancel{E}_T)$

$t\bar{t}H$

$t\bar{t}H$

$VBF \rightarrow H \rightarrow VV, t\bar{t}H, \text{new physics}$

$VBF \rightarrow H \rightarrow VV$

$t\bar{t}, \text{new physics}$

SUSY tri-lepton

ZZZ: Lazopoulos et al. '07, WWZ: Hankele et al. '08, VVV: Binoth et al. '08

Motivation

Why is $pp/p\bar{p} \rightarrow WW + \text{jet} + X$ interesting ?

- **Important background process** at the LHC (and for Tevatron Higgs searches)
“Les Houches experimenter’s wishlist ’05” for important missing NLO predictions:

process

background for

$pp \rightarrow WW + \text{jet}$

$H + \text{jet}, t\bar{t}H, \text{ new physics (leptons} + \cancel{E}_T)$

Dittmaier/S.K./Uwer '07, Campbell/Ellis/Zanderighi '07

Binoth/Guillet/Karg/Kauer/Sanguinetti (in progress)

$pp \rightarrow t\bar{t}b\bar{b}$

$t\bar{t}H$

$pp \rightarrow t\bar{t} + 2\text{jets}$

$t\bar{t}H$

$pp \rightarrow VVb\bar{b}$

$VBF \rightarrow H \rightarrow VV, t\bar{t}H, \text{ new physics}$

$pp \rightarrow VV + 2\text{jets}$

$VBF \rightarrow H \rightarrow VV$

VBF: Jäger et al. '06, Bozzi et al. '07

$pp \rightarrow V + 3\text{jets}$

$t\bar{t}, \text{ new physics}$

$pp \rightarrow VVV$

SUSY tri-lepton

ZZZ: Lazopoulos et al. '07, WWZ: Hankele et al. '08, VVV: Binoth et al. '08

- A large fraction of W-pair events at the LHC show additional jet activity.
↔ **EW gauge-boson coupling analysis**

Motivation

Why is $pp/p\bar{p} \rightarrow WW + \text{jet} + X$ interesting ?

- **Important background process** at the LHC (and for Tevatron Higgs searches)
“Les Houches experimenter’s wishlist ’05” for important missing NLO predictions:

process

background for

$pp \rightarrow WW + \text{jet}$

$H + \text{jet}, t\bar{t}H$, new physics (leptons + \cancel{E}_T)

Dittmaier/S.K./Uwer '07, Campbell/Ellis/Zanderighi '07

Binoth/Guillet/Karg/Kauer/Sanguinetti (in progress)

$pp \rightarrow t\bar{t}b\bar{b}$

$t\bar{t}H$

$pp \rightarrow t\bar{t} + 2\text{jets}$

$t\bar{t}H$

$pp \rightarrow VVb\bar{b}$

$VBF \rightarrow H \rightarrow VV, t\bar{t}H$, new physics

$pp \rightarrow VV + 2\text{jets}$

$VBF \rightarrow H \rightarrow VV$

VBF: Jäger et al. '06, Bozzi et al. '07

$pp \rightarrow V + 3\text{jets}$

$t\bar{t}$, new physics

$pp \rightarrow VVV$

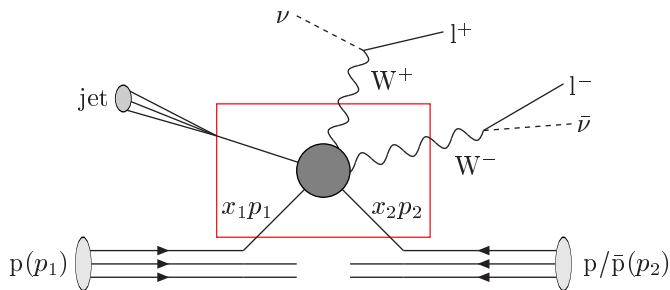
SUSY tri-lepton

ZZZ: Lazopoulos et al. '07, WWZ: Hankele et al. '08, VVV: Binoth et al. '08

- A large fraction of W-pair events at the LHC show additional jet activity.
↔ **EW gauge-boson coupling analysis**
- Process is an **important test ground** before approaching more complicated many-particle processes at NLO.

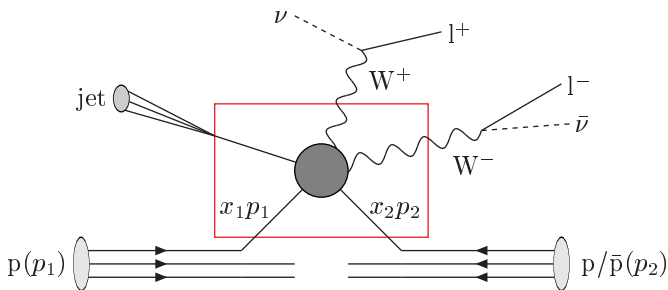
Hadronic cross section

Schematic illustration of the hadronic process $pp/p\bar{p} \rightarrow W^+W^- + \text{jet} + X$:



Hadronic cross section

Schematic illustration of the hadronic process $pp/p\bar{p} \rightarrow W^+W^- + \text{jet} + X$:



Hadronic cross section:

$$\sigma^{pp/p\bar{p}}(p_1, p_2) = \sum_{a,b} \int_0^1 dx_1 \int_0^1 dx_2 \underbrace{f_{a(p)}(x_1, \mu_F) f_{b(p/\bar{p})}(x_2, \mu_F)}_{\text{PDF's of parton } a/b \text{ in } p/\bar{p}} \underbrace{\hat{\sigma}^{ab}(x_1 p_1, x_2 p_2)}_{\text{partonic cross section}}$$

Treatment of quarks

All light quarks (u, d, s, c, b) are treated as massless particles.

↔ IR singularities are treated in dimensional regularization.

Treatment of quarks

All light quarks (u, d, s, c, b) are treated as massless particles.

↪ IR singularities are treated in dimensional regularization.

For external particles only the two light generations (u, d, s, c) are taken into account.

- initial state: negligible contributions due to small b-quark pdf's
- final state: selection by anti-b-tagging

Treatment of quarks

All light quarks (u, d, s, c, b) are treated as massless particles.

↪ IR singularities are treated in dimensional regularization.

For external particles only the two light generations (u, d, s, c) are taken into account.

- initial state: negligible contributions due to small b-quark pdf's
- final state: selection by anti-b-tagging

The CKM matrix reduces to Cabibbo matrix (mixing only between the two light generations). Many subprocesses are not influenced by CKM matrix (unitarity).

Treatment of quarks

All light quarks (u, d, s, c, b) are treated as massless particles.

↪ IR singularities are treated in dimensional regularization.

For external particles only the two light generations (u, d, s, c) are taken into account.

- initial state: negligible contributions due to small b-quark pdf's
- final state: selection by anti-b-tagging

The CKM matrix reduces to Cabibbo matrix (mixing only between the two light generations). Many subprocesses are not influenced by CKM matrix (unitarity).

The running of α_S is solely generated by light quark and gluon loops.
(The top-quark loop is subtracted at zero momentum.)

↪ 5-flavour-running of α_S

Subprocesses contributing at leading order

6 partonic channels in LO (12 flavour channels for 2 generations, b quarks negligible):

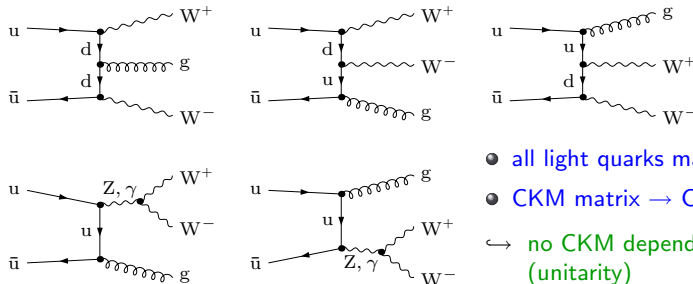
$$\begin{aligned} u\bar{u} &\rightarrow W^+W^-g, & ug &\rightarrow W^+W^-u, & g\bar{u} &\rightarrow W^+W^-\bar{u}, \\ d\bar{d} &\rightarrow W^+W^-g, & dg &\rightarrow W^+W^-d, & g\bar{d} &\rightarrow W^+W^-\bar{d} \end{aligned}$$

Subprocesses contributing at leading order

6 partonic channels in LO (12 flavour channels for 2 generations, b quarks negligible):

$$\begin{aligned}
 u\bar{u} &\rightarrow W^+W^-g, & ug &\rightarrow W^+W^-u, & g\bar{u} &\rightarrow W^+W^-\bar{u}, \\
 d\bar{d} &\rightarrow W^+W^-g, & dg &\rightarrow W^+W^-d, & g\bar{d} &\rightarrow W^+W^-\bar{d}
 \end{aligned}$$

Diagrams for $u\bar{u}$ initial state:



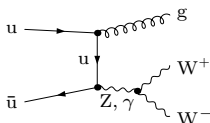
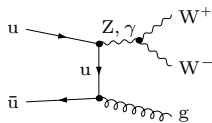
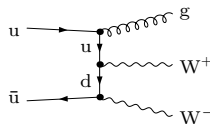
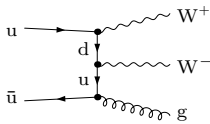
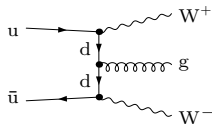
- all light quarks massless
- CKM matrix \rightarrow Cabibbo matrix
- \hookrightarrow no CKM dependence in LO (unitarity)

Subprocesses contributing at leading order

6 partonic channels in LO (12 flavour channels for 2 generations, b quarks negligible):

$$\begin{aligned} u\bar{u} &\rightarrow W^+W^-g, & ug &\rightarrow W^+W^-u, & g\bar{u} &\rightarrow W^+W^-\bar{u}, \\ d\bar{d} &\rightarrow W^+W^-g, & dg &\rightarrow W^+W^-d, & g\bar{d} &\rightarrow W^+W^-\bar{d} \end{aligned}$$

Diagrams for $u\bar{u}$ initial state:

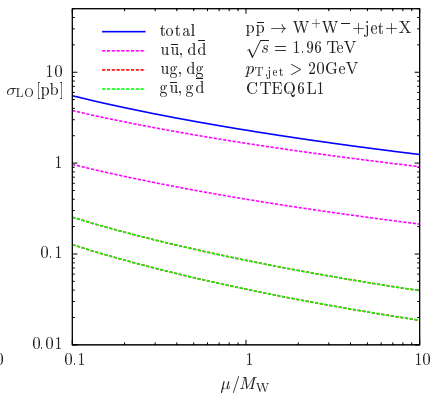
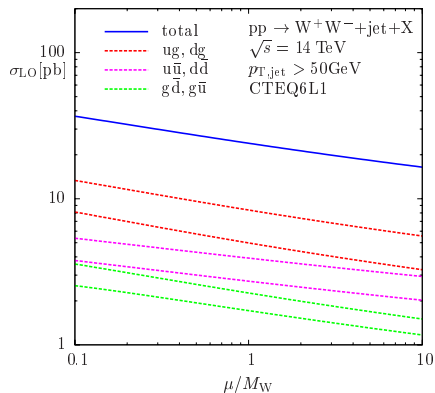


- all light quarks massless
 - CKM matrix \rightarrow Cabibbo matrix
- \hookrightarrow no CKM dependence in LO (unitarity)

The amplitudes for all other channels are generated by crossing the gluon into the initial state and by SU(2) symmetry ($u \leftrightarrow d, W^+ \leftrightarrow W^-$).

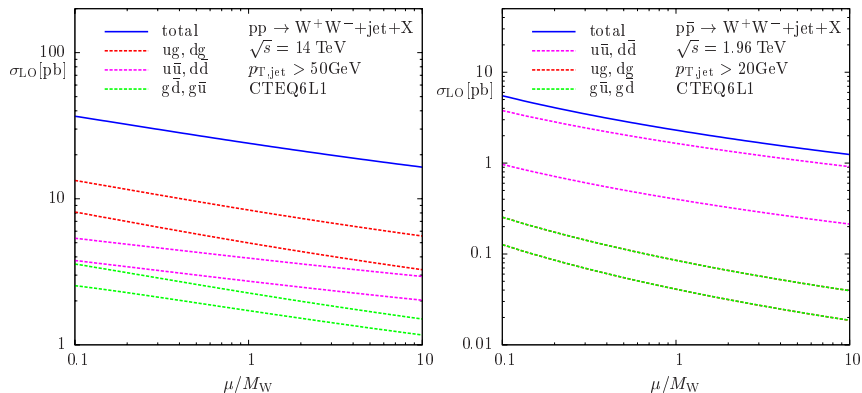
Leading-order prediction

Scale dependence of LO cross section (with $\mu = \mu_{\text{fact}} = \mu_{\text{ren}}$):



Leading-order prediction

Scale dependence of LO cross section (with $\mu = \mu_{\text{fact}} = \mu_{\text{ren}}$):



LHC: Cross section changes by 12% (30%) when scaling μ by a factor of 2 (5).

Tevatron: Cross section changes by 25% (75%) when scaling μ by a factor of 2 (5).

↪ For precise predictions the calculation of NLO QCD corrections is required.

General form of NLO QCD corrections

The NLO cross section gets contributions which are separately **IR divergent**:

- **Real corrections** (emission of another QCD parton)
- **Virtual corrections** (exchange of virtual particles)

For **jet observables** (sufficiently inclusive via jet algorithm) **factorization theorems** state:

Sum of **divergences** is **universal and connected to initial state**. \rightarrow PDF redefinition

- **Collinear-subtraction counterterm** (factorization scale dependence)

\hookrightarrow **Sum over contributions is finite.**

General form of NLO QCD corrections

The NLO cross section gets contributions which are separately **IR divergent**:

- **Real corrections** (emission of another QCD parton)
- **Virtual corrections** (exchange of virtual particles)

For **jet observables** (sufficiently inclusive via jet algorithm) **factorization theorems** state:

Sum of **divergences** is **universal and connected to initial state**. \rightarrow PDF redefinition

- **Collinear-subtraction counterterm** (factorization scale dependence)

\hookrightarrow **Sum over contributions is finite.**

But: Numerical cancellations between different phase spaces required.

Technical solution: Dipole subtraction formalism [Catani, Seymour '96]:

Add and subtract an approximation of the cross section $d\sigma^A$:

- $d\sigma^A$ exactly matches the **singular behaviour** of $d\sigma^R$ in $d = 4 - 2\epsilon$ dimensions.
- $d\sigma^A$ is integrable analytically over the single-parton subspaces in $d = 4 - 2\epsilon$ dimensions leading to **soft and collinear divergences** (like in $d\sigma^V$ and $d\sigma^C$).

NLO cross section with the dipole subtraction formalism

Schematic formula for the NLO cross section in the situation of two initial-state hadrons (LHC and Tevatron):

$$\sigma^{\text{NLO}} = \underbrace{\int_{m+1} d\sigma^R}_{\text{real corrections}} + \underbrace{\int_m d\sigma^V}_{\text{virtual corrections}} + \underbrace{\int_0^1 dx \int_m d\sigma^C}_{\text{collinear-subtraction counterterm}}$$

NLO cross section with the dipole subtraction formalism

Schematic formula for the NLO cross section in the situation of two initial-state hadrons (LHC and Tevatron):

$$\sigma^{\text{NLO}} = \underbrace{\int_{m+1} d\sigma^R}_{\text{real corrections}} + \underbrace{\int_m d\sigma^V}_{\text{virtual corrections}} + \underbrace{\int_0^1 dx \int_m d\sigma^C}_{\text{collinear-subtraction counterterm}} - \int_{m+1} d\sigma^A + \int_{m+1} d\sigma^A,$$

$$d\sigma^A = \sum_{\text{dipoles}} d\sigma^B \otimes dV_{\text{dipole}}$$

NLO cross section with the dipole subtraction formalism

Schematic formula for the NLO cross section in the situation of two initial-state hadrons (LHC and Tevatron):

$$\begin{aligned}
 \sigma^{\text{NLO}} &= \underbrace{\int_{m+1} d\sigma^R}_{\text{real corrections}} + \underbrace{\int_m d\sigma^V}_{\text{virtual corrections}} + \underbrace{\int_0^1 dx \int_m d\sigma^C}_{\text{collinear-subtraction counterterm}} - \int_{m+1} d\sigma^A + \int_{m+1} d\sigma^A, \\
 & \hspace{20em} d\sigma^A = \sum_{\text{dipoles}} d\sigma^B \otimes dV_{\text{dipole}} \\
 &= \int_{m+1} \left[d\sigma^R - d\sigma^A \right]_{\epsilon=0} \hspace{15em} \Rightarrow R - A \\
 & \quad + \int_m \left[d\sigma^V + \sum_{\text{dipoles}} d\sigma^B \otimes V_{\text{dipole}}(1) \right]_{\epsilon=0} \hspace{15em} \Rightarrow V + A \\
 & \quad + \int_0^1 dx \int_m \left[d\sigma^C + \sum_{\text{dipoles}} \int_1^x d\sigma^B(x) \otimes [dV_{\text{dipole}}(x)]_+ \right]_{\epsilon=0} \hspace{15em} \Rightarrow C + A \\
 & \hspace{10em} dV_{\text{dipole}}(x) = [dV_{\text{dipole}}(x)]_+ + dV_{\text{dipole}}(1)\delta(1-x)
 \end{aligned}$$

Virtual corrections (V+A term)

For each channel $\mathcal{O}(100)$ 1-loop diagrams contribute, which can be classified as

- “bosonic” corrections (exchange of an additional gluon)
- “fermionic” corrections (closed quark loops)

Renormalization leads to counterterm diagrams contributing at the 1-loop level.

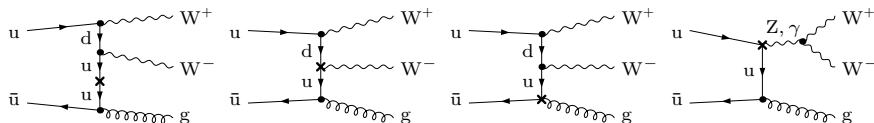
Virtual corrections (V+A term)

For each channel $\mathcal{O}(100)$ 1-loop diagrams contribute, which can be classified as

- “bosonic” corrections (exchange of an additional gluon)
- “fermionic” corrections (closed quark loops)

Renormalization leads to counterterm diagrams contributing at the 1-loop level.

Representative sample of counterterm diagrams:



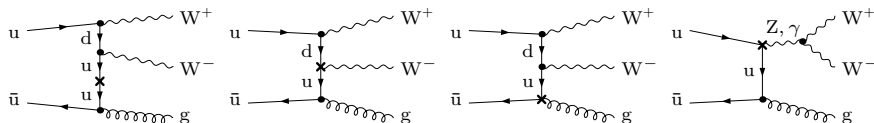
Virtual corrections (V+A term)

For each channel $\mathcal{O}(100)$ 1-loop diagrams contribute, which can be classified as

- “bosonic” corrections (exchange of an additional gluon)
- “fermionic” corrections (closed quark loops)

Renormalization leads to counterterm diagrams contributing at the 1-loop level.

Representative sample of counterterm diagrams:



Sum over all counterterm diagrams is proportional to tree-level amplitude:

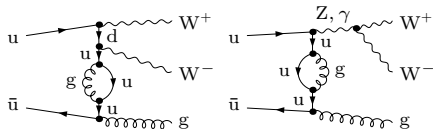
$$\mathcal{M}_{\text{born}} \times \frac{\alpha_s}{4\pi} \left[\underbrace{-\frac{13}{3} \Delta_{\text{UV}}(\mu) - \frac{7}{6} \Delta_{\text{IR}}(\mu) + \frac{N_f}{3} \Delta_{\text{IR}}(\mu)}_{\text{cancel against loops or real corrections}} + \underbrace{\left(\frac{11}{2} - \frac{N_f}{3} \right)}_{\propto \beta(\alpha_s)} \log \frac{\mu^2}{M_W^2} \right],$$

$$\Delta_{\text{IR}}(\mu) = \frac{\Gamma(1 + \varepsilon_{\text{IR}})}{\varepsilon_{\text{IR}}} \left(\frac{4\pi\mu^2}{M_W^2} \right)^{\varepsilon_{\text{IR}}}, \quad \Delta_{\text{UV}}(\mu) = \frac{\Gamma(1 + \varepsilon_{\text{UV}})}{\varepsilon_{\text{UV}}} \left(\frac{4\pi\mu^2}{M_W^2} \right)^{\varepsilon_{\text{UV}}}$$

Virtual corrections (V+A term)

Bosonic corrections can be further subdivided to

- self-energy contributions (2-point functions)

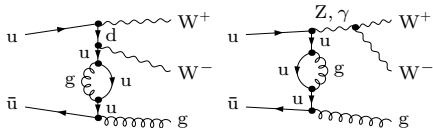


$$\mathcal{M}_{\text{self-energy}} \overset{\text{UV}}{\sim} \int d^4 q \frac{q^\mu}{(q^2)^2} \sim \int_0^\infty d|q| \rightarrow \text{UV-divergent, but IR-finite}$$

Virtual corrections (V+A term)

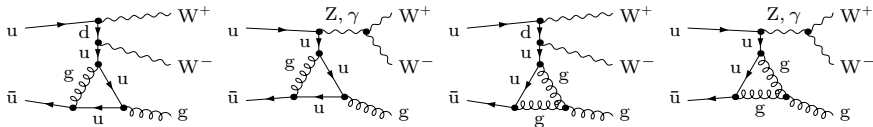
Bosonic corrections can be further subdivided to

- self-energy contributions (2-point functions)



$$\mathcal{M}_{\text{self-energy}} \overset{\text{UV}}{\sim} \int d^4 q \frac{q^\mu}{(q^2)^2} \sim \int_0^\infty d|q| \rightarrow \text{UV-divergent, but IR-finite}$$

- vertex contributions (3-point functions)

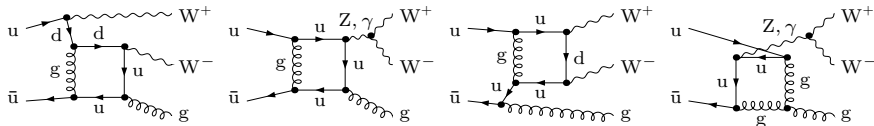


$$\mathcal{M}_{\text{vertex}} \overset{\text{UV}}{\sim} \int d^4 q \frac{q^\mu q^\nu}{(q^2)^3} \sim \int_0^\infty d|q| |q|^{-1} \rightarrow \text{UV-divergent, also IR-divergent}$$

Virtual corrections (V+A term)

Further **bosonic corrections**:

- **box contributions** (4-point functions)

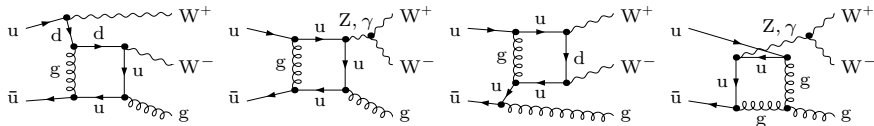


$$\mathcal{M}_{\text{box}} \overset{\text{UV}}{\sim} \int d^4 q \frac{q^\mu q^\nu q^\rho}{(q^2)^4} \sim \int_0^\infty d|q| |q|^{-2} \rightarrow \text{UV-finite, but IR-divergent}$$

Virtual corrections (V+A term)

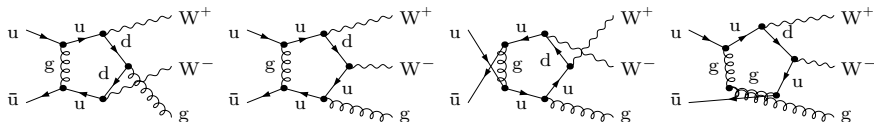
Further **bosonic corrections**:

- **box contributions** (4-point functions)



$$\mathcal{M}_{\text{box}}^{\text{UV}} \sim \int d^4q \frac{q^\mu q^\nu q^\rho}{(q^2)^4} \sim \int_0^\infty d|q| |q|^{-2} \rightarrow \text{UV-finite, but IR-divergent}$$

- **pentagon contributions** (5-point functions)



$$\mathcal{M}_{\text{pentagon}}^{\text{UV}} \sim \int d^4q \frac{q^\mu q^\nu q^\rho q^\sigma}{(q^2)^5} \sim \int_0^\infty d|q| |q|^{-3} \rightarrow \text{UV-finite, but IR-divergent}$$

Virtual corrections (V+A term)

Strategy for extracting or translating IR (soft / collinear) singularities

Idea: integrals $I^{(\epsilon)}$ in $d = 4 - 2\epsilon$ dim. \leftrightarrow 4-dim. integrals $I^{(\lambda)}$ with mass regulator λ

Procedure: Consider finite and regularization-scheme-independent difference:

$$\begin{aligned} \left[I^{(\epsilon)} - I_{\text{sing}}^{(\epsilon)} \right] \Big|_{\epsilon \rightarrow 0} &= \left[I^{(\lambda)} - I_{\text{sing}}^{(\lambda)} \right] \Big|_{\lambda \rightarrow 0} \\ \Rightarrow I^{(\epsilon)} &= I_{\text{sing}}^{(\epsilon)} + \left[I^{(\lambda)} - I_{\text{sing}}^{(\lambda)} \right] \Big|_{\lambda \rightarrow 0} + \mathcal{O}(\epsilon) \end{aligned}$$

Virtual corrections (V+A term)

Strategy for extracting or translating IR (soft / collinear) singularities

Idea: integrals $I^{(\epsilon)}$ in $d = 4 - 2\epsilon$ dim. \leftrightarrow 4-dim. integrals $I^{(\lambda)}$ with mass regulator λ

Procedure: Consider finite and regularization-scheme-independent difference:

$$\left[I^{(\epsilon)} - I_{\text{sing}}^{(\epsilon)} \right] \Big|_{\epsilon \rightarrow 0} = \left[I^{(\lambda)} - I_{\text{sing}}^{(\lambda)} \right] \Big|_{\lambda \rightarrow 0}$$

$$\Rightarrow I^{(\epsilon)} = I_{\text{sing}}^{(\epsilon)} + \left[I^{(\lambda)} - I_{\text{sing}}^{(\lambda)} \right] \Big|_{\lambda \rightarrow 0} + \mathcal{O}(\epsilon)$$

Note: Mass-singular part can be universally constructed from 3-point integrals.

\hookrightarrow general result known explicitly [Dittmaier '03]

[Beenakker et al. '02]

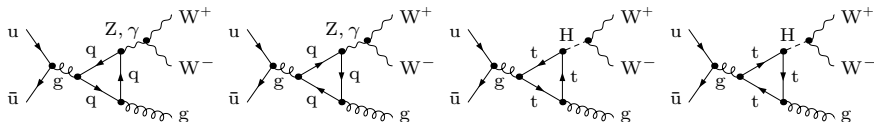
$$\left. \begin{aligned} & \left[\text{Diagram} \right]_{\text{sing}} = \left[\text{Diagram 1} \right] + \left[\text{Diagram 2} \right] \\ & + \left[\text{Diagram 3} \right] + \left[\text{Diagram 4} \right] + \left[\text{Diagram 5} \right] \end{aligned} \right\} \begin{aligned} & \frac{1}{\epsilon^2}, \frac{1}{\epsilon} \\ & \ln^2 \lambda, \ln \lambda \end{aligned}$$

$$\left. \begin{aligned} & + \left[\text{Diagram 6} \right] + \left[\text{Diagram 7} \right] + \left[\text{Diagram 8} \right] + \left[\text{Diagram 9} \right] + \left[\text{Diagram 10} \right] \end{aligned} \right\} \begin{aligned} & \frac{1}{\epsilon} \\ & \ln \lambda \end{aligned}$$

Virtual corrections (V+A term)

Fermionic corrections can be subdivided to

- vertex contributions (3-point functions)

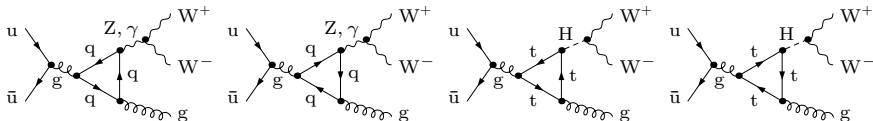


→ UV-finite because no $Zgg, \gamma gg, Hgg$ vertex exists in LO, also IR-finite

Virtual corrections (V+A term)

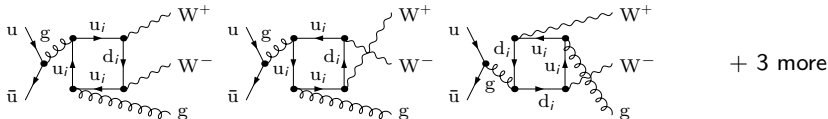
Fermionic corrections can be subdivided to

- **vertex contributions** (3-point functions)



→ UV-finite because no $Zgg, \gamma gg, Hgg$ vertex exists in LO, also IR-finite

- **box contributions** (4-point functions)



→ UV-finite (no $ggWW$ vertex in LO), also IR-finite

Virtual corrections (V+A term)

Two different strategies for evaluation of loop amplitudes
(realized in two independent calculations!)

- Analogous to NLO calculation for $pp \rightarrow t\bar{t}H$ [Beenakker et al. '02] and $pp \rightarrow t\bar{t} + \text{jet}$ [Dittmaier, Uwer, Weinzierl '07]
 - diagrams generated with FEYNARTS 1.0 [Küblbeck, Böhm, Denner '90] and reduced with in-house MATHEMATICA routines \rightarrow FORTRAN
 - analytical extraction of IR singularities [Beenakker et al. '02, Dittmaier '03]
 - reduction of 5-point to 4-point integrals according to [Denner, Dittmaier '02]

Virtual corrections (V+A term)

Two different strategies for evaluation of loop amplitudes
(realized in two independent calculations!)

- Analogous to NLO calculation for $pp \rightarrow t\bar{t}H$ [Beenakker et al. '02] and $pp \rightarrow t\bar{t} + \text{jet}$ [Dittmaier, Uwer, Weinzierl '07]
 - diagrams generated with FEYNARTS 1.0 [Küblbeck, Böhm, Denner '90] and reduced with in-house MATHEMATICA routines \rightarrow FORTRAN
 - analytical extraction of IR singularities [Beenakker et al. '02, Dittmaier '03]
 - reduction of 5-point to 4-point integrals according to [Denner, Dittmaier '02]
- Alternative calculation with available tools
 - diagrams generated with FEYNARTS 3.2 [Hahn '00]
 - algebraic reduction / numerical evaluation with FORMCALC 5.2/LOOPTOOLS: [Hahn, Perez-Victoria '98]
 - reduction of 5-point integrals à la [Denner, Dittmaier '02]
 - regular scalar integrals with FF [v.Oldenborgh '91]
 - dimensionally regularized singular integrals implemented into LOOPTOOLS:
 - box integrals checked against result of [Bern, Dixon, Kosower '93]

Real corrections (R–A term)

Contributing processes are generated by two types of generic amplitudes,

- $0 \rightarrow W^+W^-q\bar{q}gg$,
- $0 \rightarrow W^+W^-q\bar{q}q'\bar{q}'$,

and crossing any two partons into the initial state.

↪ Large number of contributions (136 flavour channels for 2 generations)!

Real corrections (R–A term)

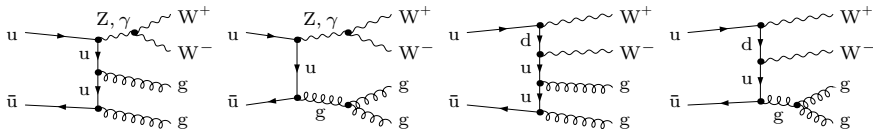
Contributing processes are generated by two types of generic amplitudes,

- $0 \rightarrow W^+W^-q\bar{q}g$,
- $0 \rightarrow W^+W^-q\bar{q}q'\bar{q}'$,

and crossing any two partons into the initial state.

↪ Large number of contributions (136 flavour channels for 2 generations)!

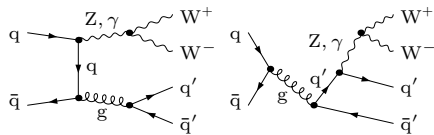
Representative diagrams of the subprocess $u\bar{u} \rightarrow W^+W^-gg$ (31 diagrams in total):



- Amplitudes for $ug \rightarrow W^+W^-ug$, $g\bar{u} \rightarrow W^+W^-g\bar{u}$ and $gg \rightarrow W^+W^-u\bar{u}$ are achieved from this amplitude by applying crossing symmetry.
- Amplitudes with external d-type quarks are generated via SU(2) symmetry ($u \leftrightarrow d, W^+ \leftrightarrow W^-$).

Real corrections (R–A term)

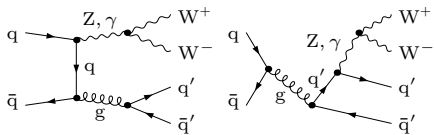
Sample of diagrams of the subprocesses $q\bar{q} \rightarrow W^+W^-q'\bar{q}'$ (up to 28 diagrams):



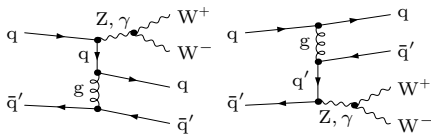
$u\bar{u} \rightarrow W^+W^-c\bar{c}$, $u\bar{u} \rightarrow W^+W^-d\bar{d}$, ...

Real corrections (R-A term)

Sample of diagrams of the subprocesses $q\bar{q} \rightarrow W^+W^-q'\bar{q}'$ (up to **28 diagrams**):



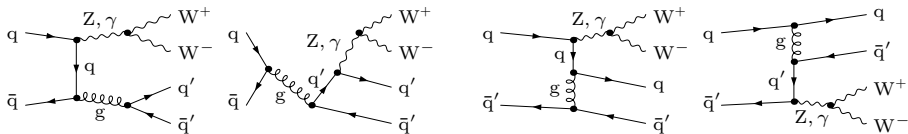
$u\bar{u} \rightarrow W^+W^-c\bar{c}, u\bar{u} \rightarrow W^+W^-d\bar{d}, \dots$



$u\bar{c} \rightarrow W^+W^-u\bar{c}, u\bar{d} \rightarrow W^+W^-u\bar{d}, \dots$

Real corrections (R–A term)

Sample of diagrams of the subprocesses $q\bar{q} \rightarrow W^+W^-q'\bar{q}'$ (up to **28 diagrams**):



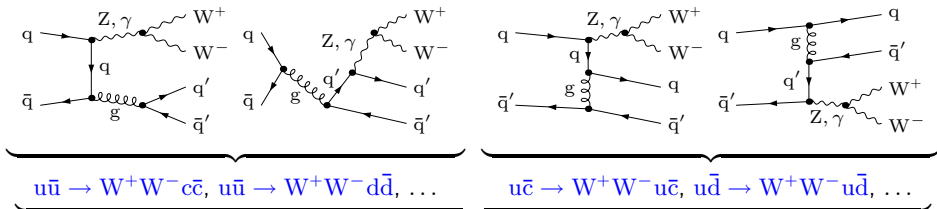
$u\bar{u} \rightarrow W^+W^-c\bar{c}, u\bar{u} \rightarrow W^+W^-d\bar{d}, \dots$

$u\bar{c} \rightarrow W^+W^-u\bar{c}, u\bar{d} \rightarrow W^+W^-u\bar{d}, \dots$

$u\bar{u} \rightarrow W^+W^-u\bar{u}, d\bar{d} \rightarrow W^+W^-d\bar{d}, \dots$

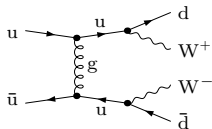
Real corrections (R–A term)

Sample of diagrams of the subprocesses $q\bar{q} \rightarrow W^+W^-q'\bar{q}'$ (up to **28 diagrams**):



$$u\bar{u} \rightarrow W^+W^-u\bar{u}, d\bar{d} \rightarrow W^+W^-d\bar{d}, \dots$$

Further diagrams contribute in case of **both external u-type and d-type quarks**:



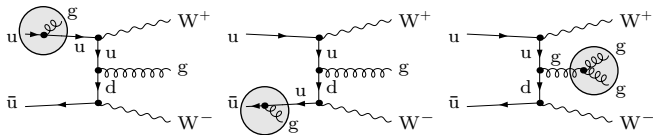
W bosons couple to different fermion lines.

↪ Subprocesses with up to 4 different quark flavours give non-vanishing contributions (e. g. $u\bar{c} \rightarrow W^+W^-d\bar{s}$).

Crossing symmetry leads to amplitudes for the subprocess classes $qq \rightarrow W^+W^-qq$ and $\bar{q}\bar{q} \rightarrow W^+W^-\bar{q}\bar{q}$.

Real corrections (R–A term)

For $u\bar{u} \rightarrow W^+W^-gg$ IR singularities are cured by the following subtraction terms:

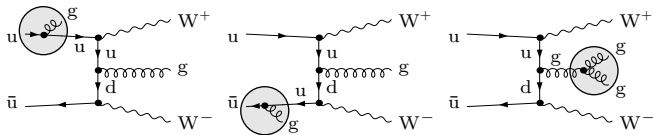


- process-independent part \rightarrow dipole terms \rightarrow IR (soft and collinear) singularities
- process-dependent part \rightarrow on-shell amplitudes of LO subprocesses

Note: Spin and colour correlations have to be taken into account.

Real corrections (R–A term)

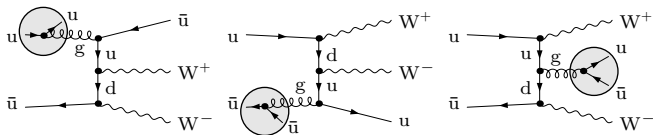
For $u\bar{u} \rightarrow W^+W^-gg$ IR singularities are cured by the following subtraction terms:



- process-independent part \rightarrow dipole terms \rightarrow IR (soft and collinear) singularities
- process-dependent part \rightarrow on-shell amplitudes of LO subprocesses

Note: Spin and colour correlations have to be taken into account.

E. g. for $u\bar{u} \rightarrow W^+W^-u\bar{u}$ subtraction terms contain different $2 \rightarrow 3$ -subprocesses:



Real corrections (R–A term)

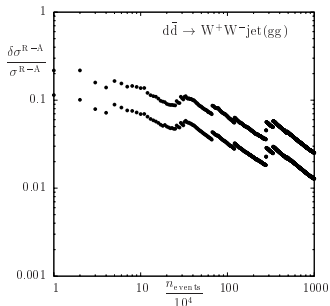
Subtraction-term phase spaces have the following features:

- **Momentum conservation** is maintained.
- A **one-to-one-correspondence** between subtraction-term phase space and real-correction phase space exists (degenerate in the relevant limits).

Numerical problem:

R – **A**

event passes cuts event is cut away (or vice versa)



Real corrections (R–A term)

Subtraction-term phase spaces have the following features:

- **Momentum conservation** is maintained.
- A **one-to-one-correspondence** between subtraction-term phase space and real-correction phase space exists (degenerate in the relevant limits).

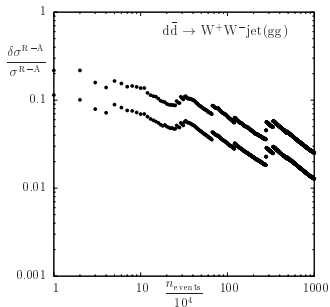
Numerical problem:

R – A

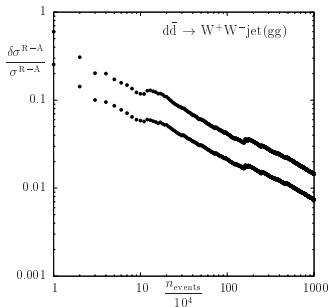
event passes cuts

event is cut away

(or vice versa)



Improved numerical integration by adding extra channels populating the critical region:



Real corrections (R–A term)

Two independent evaluations of helicity amplitudes:

- application of (4-dimensional) WvdW spinor techniques
- alternative evaluation based on MADGRAPH [Stelzer, Long '94]

Real corrections (R–A term)

Two independent evaluations of helicity amplitudes:

- application of (4-dimensional) WvdW spinor techniques
- alternative evaluation based on MADGRAPH [Stelzer, Long '94]

Two independent versions of Monte Carlo integrators:

- one entirely based on multi-channel MC technique [Berends, Pittau, Kleis '94] [Kleis, Pittau '94]
- non-singular parts checked against SHERPA 1.0.8 [Gleisberg et al. '03] and WHIZARD 1.50 [Kilian '01] (details on comparison → [diploma thesis of S.K. '06])

process	σ [pb]	σ_{SHERPA} [pb]	$\Delta\sigma/\text{stat. error}$
$p\bar{p} \rightarrow WW + 1\text{jet}$	2.10456(94)	2.10562(78)	-0.87
$p\bar{p} \rightarrow WW + 2\text{jets}$	0.42431(22)	0.42437(13)	-0.23
$pp \rightarrow WW + 1\text{jet}$	46.453(16)	46.4399(94)	+0.70
$pp \rightarrow WW + 2\text{jets}$	31.555(17)	31.5747(63)	-1.08

- extra channels included for subtraction terms
- second version based on simple mapping (phase space by sequential splitting)

Collinear subtraction counterterm (C+A term)

Incoming hadrons require collinear subtraction counterterms:

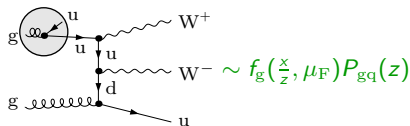
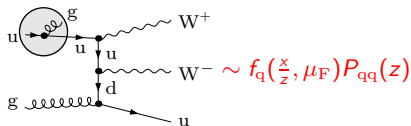
- divergences resulting from collinear emission off these identified partons
↔ no cancellation against virtual corrections
- absorption of divergences in redefined parton distribution functions (PDF's)

Collinear subtraction counterterm (C+A term)

Incoming hadrons require collinear subtraction counterterms:

- divergences resulting from collinear emission off these identified partons
 \hookrightarrow no cancellation against virtual corrections
- absorption of divergences in redefined parton distribution functions (PDF's)

Sample of diagrams showing collinear subtraction counterterms:



Corresponding redefinition of PDF's:

$P_{ij}(z) =$ Altarelli–Parisi splitting functions

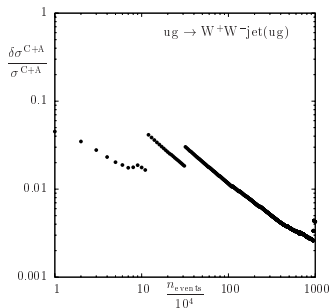
$$\begin{aligned}
 f_q(x, \mu_F) &\rightarrow f_q(x, \mu_F) \\
 &+ \frac{\alpha_s}{2\pi} \int_x^1 \frac{dz}{z} f_q\left(\frac{x}{z}, \mu_F\right) \left(\frac{\Gamma(1+\varepsilon)}{\varepsilon} (4\pi)^\varepsilon + \ln \frac{\mu^2}{\mu_F^2} \right) C_F [P_{qq}(z)]_+ \\
 &+ \frac{\alpha_s}{2\pi} \int_x^1 \frac{dz}{z} f_g\left(\frac{x}{z}, \mu_F\right) \left(\frac{\Gamma(1+\varepsilon)}{\varepsilon} (4\pi)^\varepsilon + \ln \frac{\mu^2}{\mu_F^2} \right) T_R P_{gq}(z) \\
 f_g(x, \mu_F) &\rightarrow \dots \text{ analogously}
 \end{aligned}$$

Collinear subtraction counterterm (C+A term)

Meaning of z : Momentum fraction of the radiating parton after splitting

$$\int_0^1 dz \hat{\sigma}(z\hat{s}) [\mathcal{V}(z)]_+ = \int_0^1 dz \left[\hat{\sigma}(z\hat{s}) - \hat{\sigma}(\hat{s}) \right] \mathcal{V}(z)$$

- Cancellations between different phase-space points (degenerate only for $z \rightarrow 1$)!
- Spoiled cancellations if only one point passes phase-space cuts!

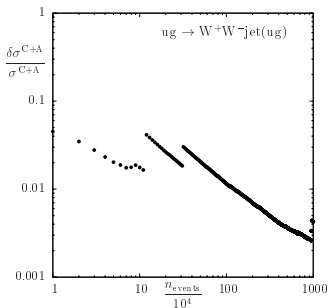


Collinear subtraction counterterm (C+A term)

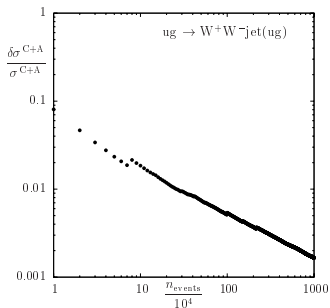
Meaning of z : Momentum fraction of the radiating parton after splitting

$$\int_0^1 dz \hat{\sigma}(z\hat{s}) [\mathcal{V}(z)]_+ = \int_0^1 dz [\hat{\sigma}(z\hat{s}) - \hat{\sigma}(\hat{s})] \mathcal{V}(z)$$

- Cancellations between different phase-space points (degenerate only for $z \rightarrow 1$)!
- Spoiled cancellations if only one point passes phase-space cuts!



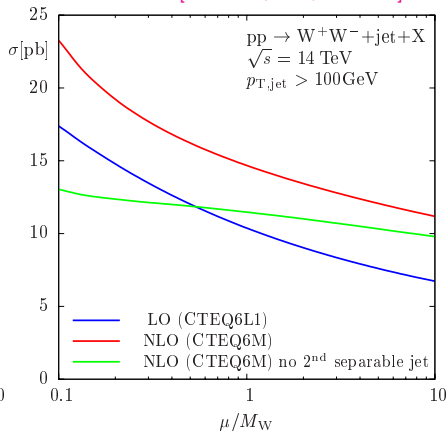
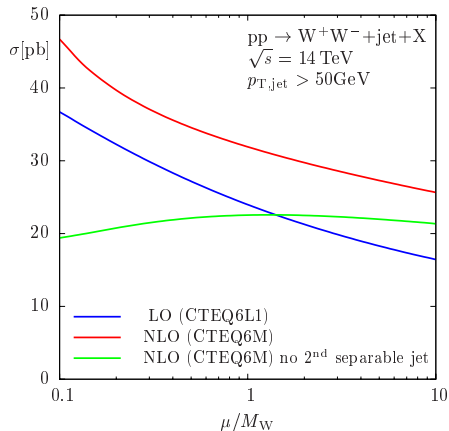
Improved numerical integration by adding extra channels populating the critical region:



Numerical results

LO versus NLO cross section at the LHC ($\mu = \mu_{\text{fact}} = \mu_{\text{ren}}$):

[Dittmaier, S.K., Uwer '07]



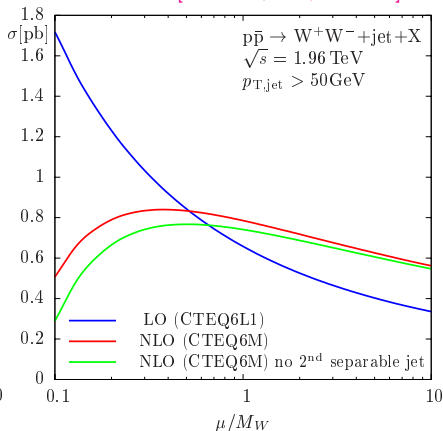
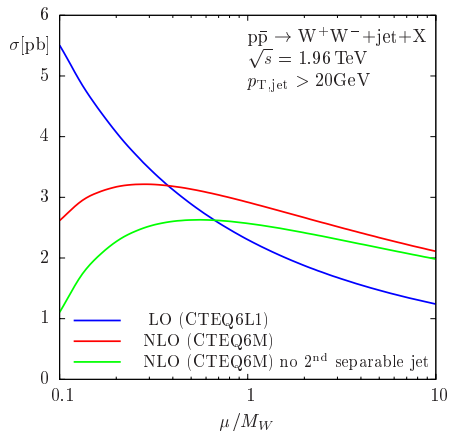
Jet definition: successive combination algorithm (with $R = 1$) [S.D.Ellis, Soper '93]

- Scale dependence stabilizes at NLO for genuine WW+jet production.
- But: Significant scale dependence is introduced by WW+2jets events.

Numerical results

LO versus NLO cross section at the Tevatron ($\mu = \mu_{\text{fact}} = \mu_{\text{ren}}$):

[Dittmaier, S.K., Uwer '07]



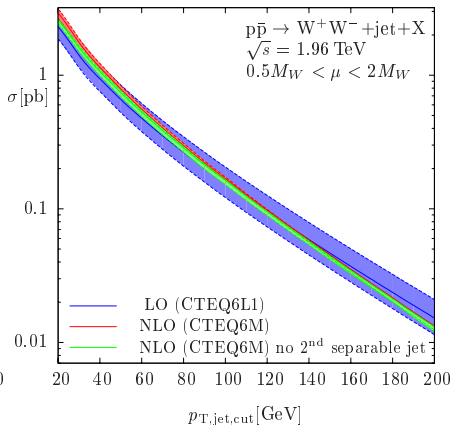
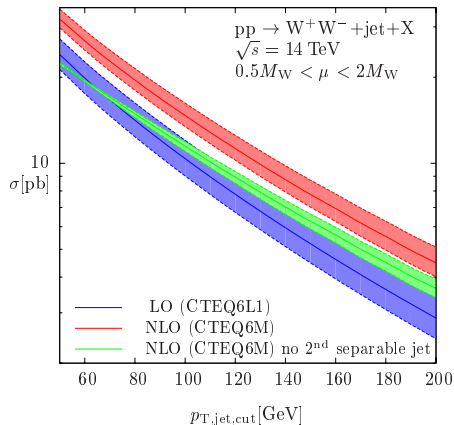
↪ Scale dependence stabilizes at NLO.
(only small influence from $WW+2\text{jets}$ production)

Numerical results

LO versus NLO cross section for $p_{T,\text{cut},\text{jet}}$ -variation at LHC and Tevatron:

($\mu = \mu_{\text{fact}} = \mu_{\text{ren}}$)

[Dittmaier, S.K., Uwer '07]



↪ Significant stabilisation of scale dependence is achieved at NLO
(at LHC especially for genuine WW+jet production)

Tuned comparison

Status of tuned comparison between results of [Dittmaier, S.K., Uwer '07], [Campbell, Ellis, Zanderighi '07] and [Binoth, Guillet, Karg, Kauer, Sanguinetti (in progress)]:

↪ [NLM Les Houches report '08]

• Integrated LO results checked:

pp → W ⁺ W ⁻ + jet + X	σ _{LO} [fb]
DKU	10371.7(12)
CEZ	10372.26(97)
BGKKS	10371.7(11)

• Results for virtual corrections checked at one phase-space point:

$$u\bar{u} \rightarrow W^+W^-g \quad |\mathcal{M}_{\text{LO}}|^2/e^4g_s^2 = 0.9963809154477200 \cdot 10^{-3}$$

$$2\text{Re}\{\mathcal{M}_V^* \cdot \mathcal{M}_{\text{LO}}\} = e^4g_s^2\Gamma(1 + \varepsilon) \left(\frac{4\pi\mu^2}{M_W^2}\right)^\varepsilon \left(\frac{1}{\varepsilon^2}c_{-2} + \frac{1}{\varepsilon}c_{-1} + c_0\right)$$

All bosonic contributions:

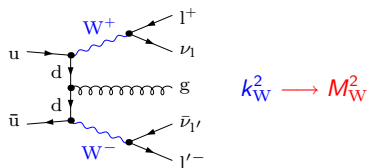
u \bar{u} → W ⁺ W ⁻ g	c ₋₂ [GeV ⁻²]	c ₋₁ ^{bos} [GeV ⁻²]	c ₀ ^{bos} [GeV ⁻²]
DKU	-1.080699305508758 · 10 ⁻⁴	7.842861905263072 · 10 ⁻⁴	-3.382910915425372 · 10 ⁻³
CEZ	-1.080699305505865 · 10 ⁻⁴	7.842861905276719 · 10 ⁻⁴	-3.382910915464027 · 10 ⁻³
BGKKS	-1.080699305508814 · 10 ⁻⁴	7.842861905263293 · 10 ⁻⁴	-3.382910915616242 · 10 ⁻³

Fermionic contributions for 2 light generations in the loop:

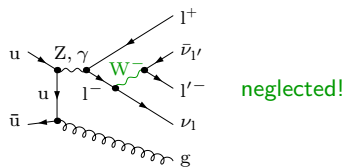
u \bar{u} → W ⁺ W ⁻ g	c ₋₁ ^{ferm1+2} [GeV ⁻²]	c ₀ ^{ferm1+2} [GeV ⁻²]
DKU	2.542821895320379 · 10 ⁻⁵	4.372323372044527 · 10 ⁻⁷
CEZ	2.542821895311753 · 10 ⁻⁵	4.372790378087550 · 10 ⁻⁷
BGKKS	2.542821895314862 · 10 ⁻⁵	4.372324288356448 · 10 ⁻⁷

W decays via narrow-width approximation

Double-resonant diagrams:

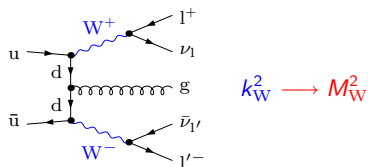


Single-resonant diagrams:

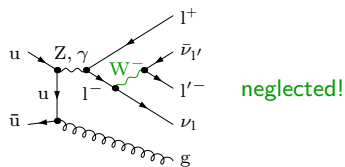


W decays via narrow-width approximation

Double-resonant diagrams:



Single-resonant diagrams:

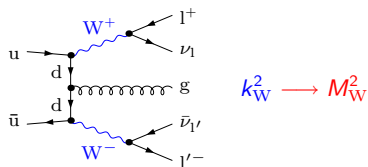


- on-shell approximation for resonant matrix elements:

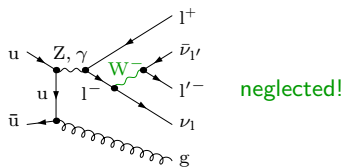
$$\mathcal{M}_{\text{resonant}} \sim \sum_{\lambda_W} \frac{\mathcal{M}_{\text{prod}}^W(k_W^2 \longrightarrow M_W^2, \lambda_W) \times \mathcal{M}_{\text{decay}}^W(k_W^2 \longrightarrow M_W^2, \lambda_W)}{k_W^2 - M_W^2 + i\Gamma_W M_W}$$

W decays via narrow-width approximation

Double-resonant diagrams:



Single-resonant diagrams:



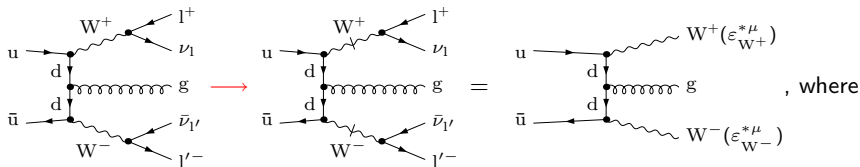
- on-shell approximation for resonant matrix elements:

$$\mathcal{M}_{\text{resonant}} \sim \sum_{\lambda_W} \frac{\mathcal{M}_{\text{prod}}^W(k_W^2 \longrightarrow M_W^2, \lambda_W) \times \mathcal{M}_{\text{decay}}^W(k_W^2 \longrightarrow M_W^2, \lambda_W)}{k_W^2 - M_W^2 + i\Gamma_W M_W}$$

- replacement of Breit–Wigner-propagator by a δ -function approximation:

$$\begin{aligned} & \int_{\min}^{\max} dk_W^2 \int d\Phi_{\text{prod}}^W(k_W^2) \frac{1}{(k_W^2 - M_W^2)^2 + \Gamma_W^2 M_W^2} \int d\Phi_{\text{decay}}^W(k_W^2) \\ \xrightarrow{\Gamma_W \rightarrow 0} & \int_{-\infty}^{\infty} dk_W^2 \int d\Phi_{\text{prod}}^W(M_W^2) \frac{\pi}{\Gamma_W M_W} \delta(k_W^2 - M_W^2) \int d\Phi_{\text{decay}}^W(M_W^2) \end{aligned}$$

W decays via narrow-width approximation

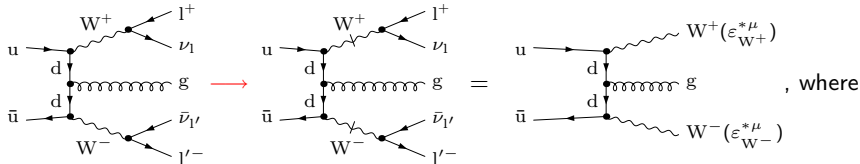


$$\epsilon_{W^+}^{*\mu} \longrightarrow \frac{1}{k_{W^+}^2 - M_W^2 + i\Gamma_W M_W} \times e C_W^- \bar{u}(k_{\nu_1}) \gamma^\mu \omega_- v(k_{l^+}), \quad k_{W^+} = k_{\nu_1} + k_{l^+}$$

$$\epsilon_{W^-}^{*\mu} \longrightarrow \underbrace{\frac{1}{k_{W^-}^2 - M_W^2 + i\Gamma_W M_W}}_{\rightarrow \text{phase-space integration}} \times e C_W^- \bar{u}(k_{l'^-}) \gamma^\mu \omega_- v(k_{\bar{\nu}_{1'}}), \quad k_{W^-} = k_{l'^-} + k_{\bar{\nu}_{1'}}$$

Spin correlations respected!

W decays via narrow-width approximation



$$\epsilon_{W^+}^{*\mu} \longrightarrow \frac{1}{k_{W^+}^2 - M_W^2 + i\Gamma_W M_W} \times e C_W^- \bar{u}(k_{\nu_l}) \gamma^\mu \omega_- v(k_{l^+}), \quad k_{W^+} = k_{\nu_l} + k_{l^+}$$

$$\epsilon_{W^-}^{*\mu} \longrightarrow \underbrace{\frac{1}{k_{W^-}^2 - M_W^2 + i\Gamma_W M_W}}_{\rightarrow \text{phase-space integration}} \times e C_W^- \bar{u}(k_{l'^-}) \gamma^\mu \omega_- v(k_{\bar{\nu}_{l'}}), \quad k_{W^-} = k_{l'^-} + k_{\bar{\nu}_{l'}}$$

Spin correlations respected!

Phase-space factorization results from the approximation:

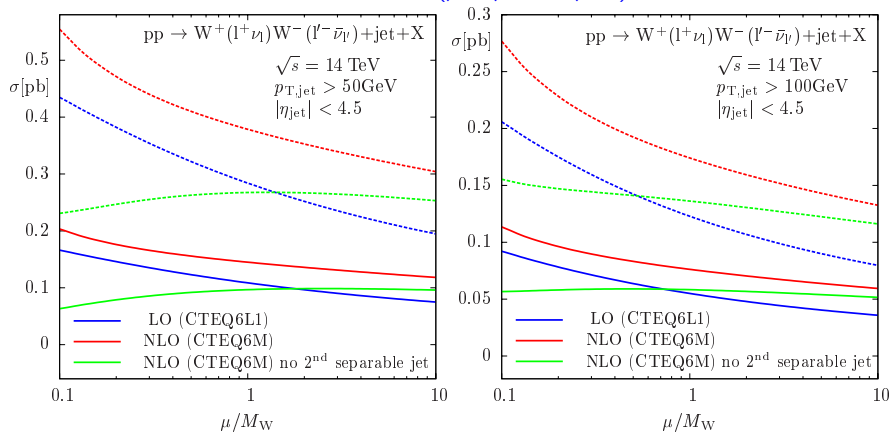
$$\int dk_{W^+}^2 \int dk_{W^-}^2 \frac{\int d\Phi_{\text{prod}}^{\text{WW}}(k_{W^+}^2, k_{W^-}^2, 0) \int d\Phi_{\text{decay}}^{\text{W}^+}(k_{W^+}^2) \int d\Phi_{\text{decay}}^{\text{W}^-}(k_{W^-}^2)}{((k_{W^+}^2 - M_W^2)^2 + \Gamma_W^2 M_W^2)((k_{W^-}^2 - M_W^2)^2 + \Gamma_W^2 M_W^2)}$$

$$\longrightarrow \left(\frac{\pi}{\Gamma_W M_W} \right)^2 \int d\Phi_{\text{prod}}^{\text{WW}}(M_W^2, M_W^2, 0) \int d\Phi_{\text{decay}}^{\text{W}^+}(M_W^2) \int d\Phi_{\text{decay}}^{\text{W}^-}(M_W^2)$$

Preliminary numerical results

LO versus NLO cross section at the LHC ($\mu = \mu_{\text{fact}} = \mu_{\text{ren}}$):

PRELIMINARY!



- Dashed lines: no leptonic cuts applied

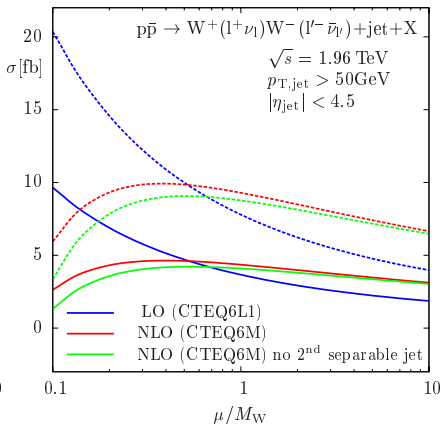
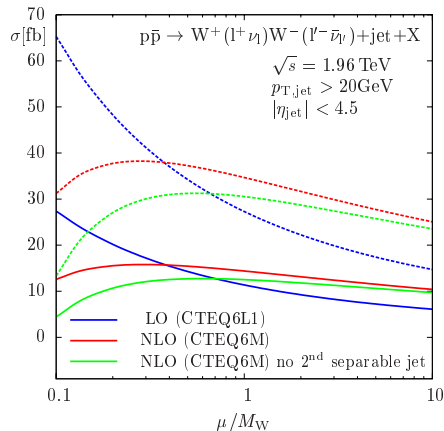
$$\hookrightarrow \sigma_{W^+(l^+\nu_l)W^-(l'\bar{\nu}_{l'})+\text{jet}} = \sigma_{W^+W^-+\text{jet}} \times (BR_{W^- \rightarrow l\nu_l})^2$$

- Solid lines: Leptonic cuts applied: $p_{T,\text{lep}} \geq 25 \text{ GeV}$, $|\eta_{\text{lep}}| \leq 2.5$, $p_{T,\text{miss}} \geq 25 \text{ GeV}$

Preliminary numerical results

LO versus NLO cross section at the Tevatron ($\mu = \mu_{\text{fact}} = \mu_{\text{ren}}$):

PRELIMINARY!



- Dashed lines: no leptonic cuts applied

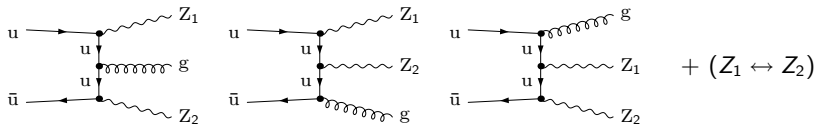
$$\hookrightarrow \sigma_{W^+(l^+\nu_l)W^-(l'\bar{\nu}_{l'})+\text{jet}} = \sigma_{W^+W^-+\text{jet}} \times (BR_{W^- \rightarrow l\nu_l})^2$$

- Solid lines: Leptonic cuts applied: $p_{T,\text{lep}} \geq 25 \text{ GeV}$, $|\eta_{\text{lep}}| \leq 2.5$, $p_{T,\text{miss}} \geq 25 \text{ GeV}$

LO subprocesses for ZZ/WZ+jet production

ZZ+jet: 6 partonic channels in LO: $u\bar{u} \rightarrow ZZg$, $ug \rightarrow ZZu$, $g\bar{u} \rightarrow ZZ\bar{u}$,
 $d\bar{d} \rightarrow ZZg$, $dg \rightarrow ZZd$, $g\bar{d} \rightarrow ZZ\bar{d}$

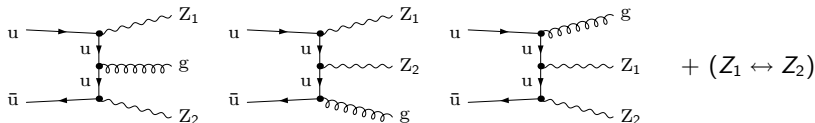
Diagrams for $u\bar{u}$ initial state:



LO subprocesses for ZZ/WZ+jet production

ZZ+jet: 6 partonic channels in LO: $u\bar{u} \rightarrow ZZg$, $ug \rightarrow ZZu$, $g\bar{u} \rightarrow ZZ\bar{u}$,
 $d\bar{d} \rightarrow ZZg$, $dg \rightarrow ZZd$, $g\bar{d} \rightarrow ZZ\bar{d}$

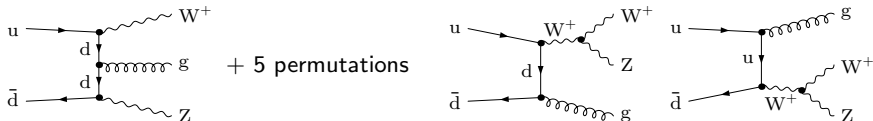
Diagrams for $u\bar{u}$ initial state:



W⁺Z+jet: 3 partonic channels in LO: $u\bar{d} \rightarrow W^+Zg$, $ug \rightarrow W^+Zd$, $g\bar{d} \rightarrow W^+Z\bar{u}$,

W⁻Z+jet: 3 partonic channels in LO: $d\bar{u} \rightarrow W^-Zg$, $dg \rightarrow W^-Zu$, $g\bar{u} \rightarrow W^-Z\bar{d}$

Diagrams for $u\bar{d}$ initial state:



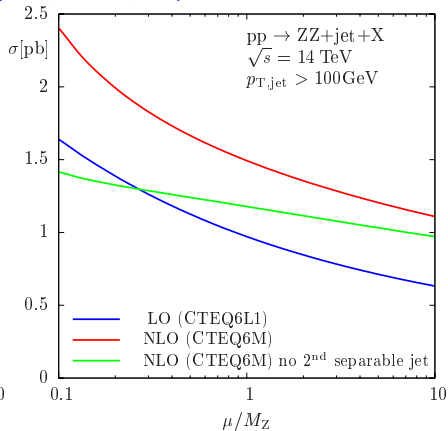
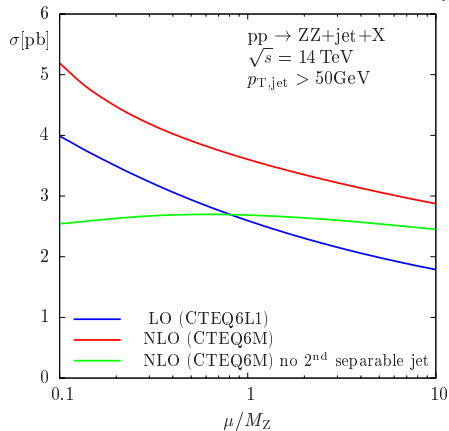
↪ explicit CKM dependence at LO for WZ+jet production

Preliminary numerical results

Similar calculation performed for $pp \rightarrow ZZ+\text{jet}+X$:

PRELIMINARY!

LO versus NLO cross section at the LHC ($\mu = \mu_{\text{fact}} = \mu_{\text{ren}}$):



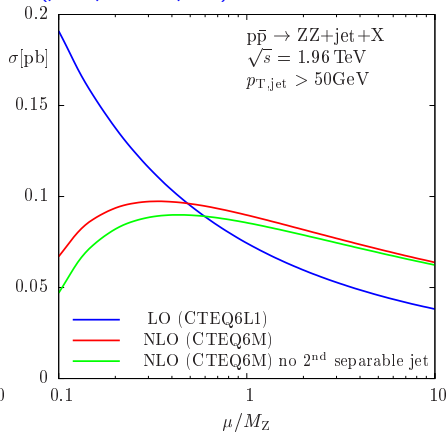
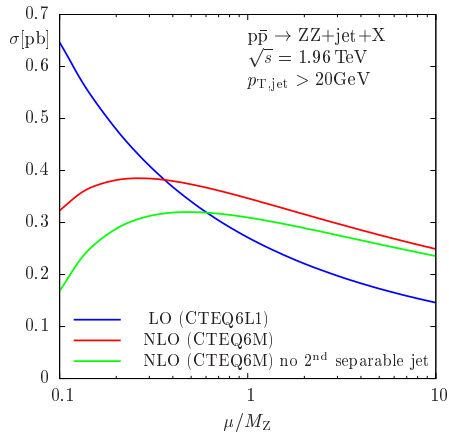
- Scale dependence stabilizes at NLO for genuine ZZ+jet production.
- But: Significant scale dependence is introduced by ZZ+2jets events.

Preliminary numerical results

Similar calculation performed for $p\bar{p} \rightarrow ZZ+\text{jet}+X$:

PRELIMINARY!

LO versus NLO cross section at the Tevatron ($\mu = \mu_{\text{fact}} = \mu_{\text{ren}}$):



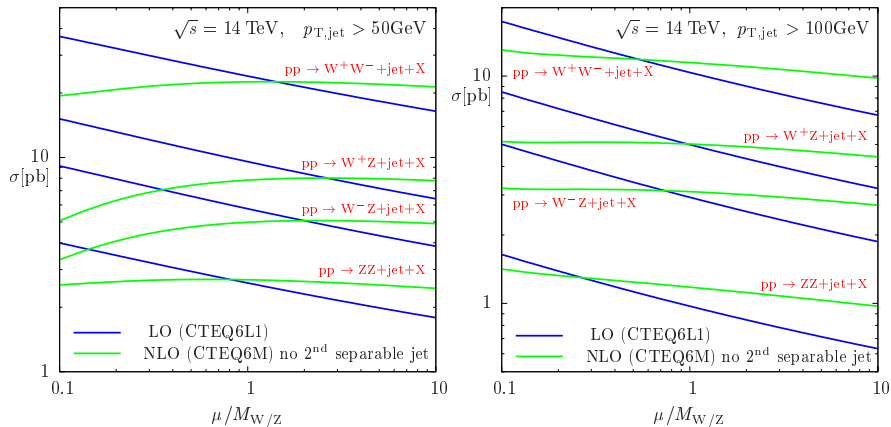
↪ Scale dependence stabilizes at NLO.
(only small influence from $ZZ+2\text{jets}$ production)

Preliminary numerical results

Summary of results for $pp \rightarrow VV + \text{jet} + X$:

PRELIMINARY!

LO versus NLO cross section at the LHC ($\mu = \mu_{\text{fact}} = \mu_{\text{ren}}$):



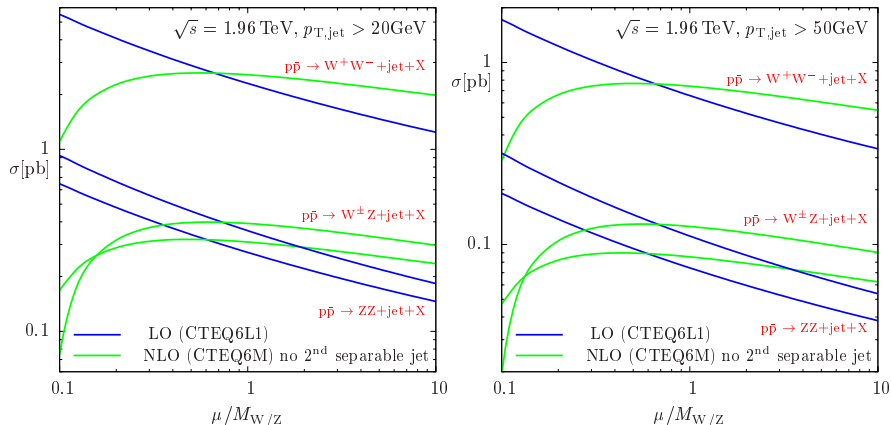
↪ Scale dependence stabilizes at NLO for genuine $VV + \text{jet}$ production.

Preliminary numerical results

Summary of results for $p\bar{p} \rightarrow VV + \text{jet} + X$:

PRELIMINARY!

LO versus NLO cross section at the Tevatron ($\mu = \mu_{\text{fact}} = \mu_{\text{ren}}$):



↪ Scale dependence stabilizes at NLO for genuine $VV + \text{jet}$ production.

Conclusions

$$pp/p\bar{p} \rightarrow WW + \text{jet} + X$$

- Important background process for Higgs and other searches at Tevatron/LHC
- WW(+jets) production used for EW gauge-boson coupling analysis at the LHC

NEW: $pp/p\bar{p} \rightarrow WW + \text{jet} + X$ at NLO QCD

- Tevatron: NLO correction stabilizes LO cross sections
- LHC: Significant reduction of scale uncertainty for genuine WW+jet production
But: significant scale dependence via WW+2jets events
- Comparison with [Ellis et al.], [Binoth et al.] in progress

Outlook & work in progress

- Implementation of leptonic W decays and distributions
- Calculation of similar processes of the class $pp/p\bar{p} \rightarrow WW/WZ/ZZ + \text{jet} + X$
- Methods not yet exhausted \rightarrow more complicated applications (2 \rightarrow 4) feasible!

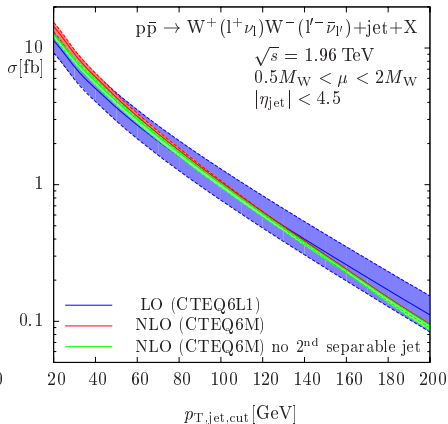
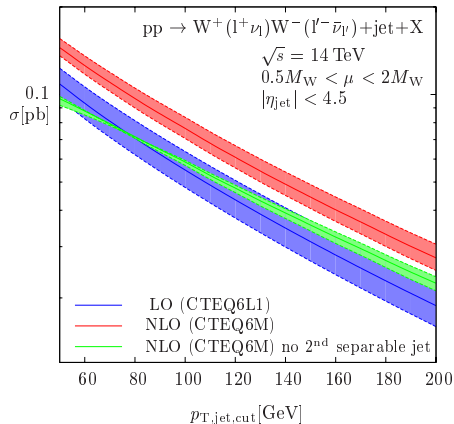
Backup slides

Preliminary numerical results

LO versus NLO cross section for $p_{T,\text{cut,jet}}$ -variation at LHC and Tevatron:

($\mu = \mu_{\text{fact}} = \mu_{\text{ren}}$)

PRELIMINARY!



Leptonic cuts applied: $p_{T,\text{lepton}} \geq 25 \text{ GeV}$, $|\eta_{\text{lepton}}| \leq 2.5$, $p_{T,\text{miss}} \geq 25 \text{ GeV}$

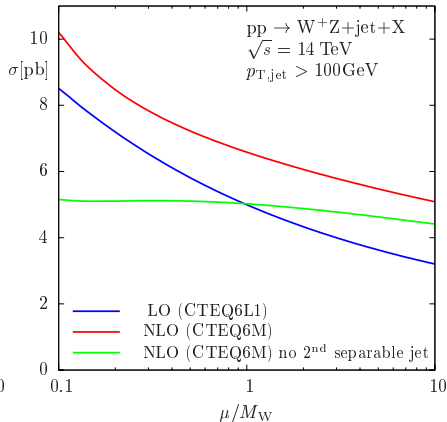
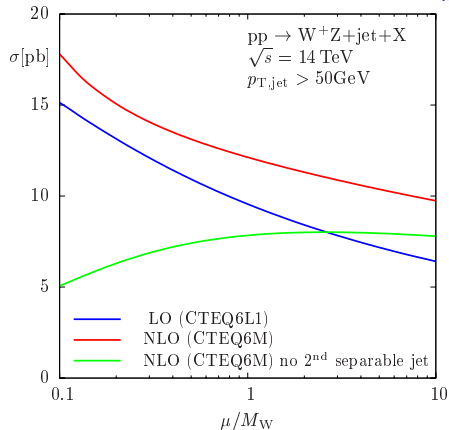
→ Significant stabilisation of scale dependence is achieved at NLO
(at LHC especially for genuine $W^+(l^+\nu_l)W^-(l'\bar{\nu}_{l'})+\text{jet}$ production)

Preliminary numerical results

Similar calculation performed for $pp \rightarrow W^+Z+\text{jet}+X$:

PRELIMINARY!

LO versus NLO cross section at the LHC ($\mu = \mu_{\text{fact}} = \mu_{\text{ren}}$):



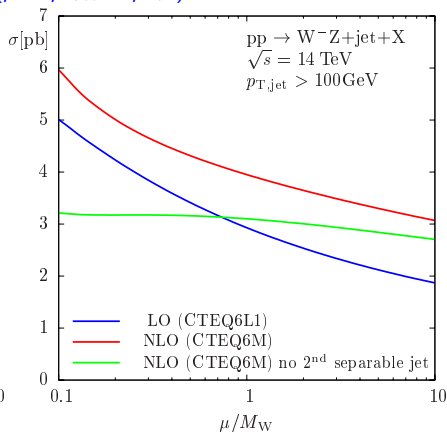
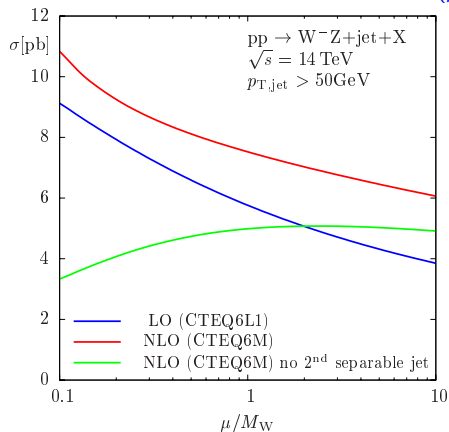
- Scale dependence stabilizes at NLO for genuine $W^+Z+\text{jet}$ production.
- But: Significant scale dependence is introduced by $W^+Z+2\text{jets}$ events.

Preliminary numerical results

Similar calculation performed for $pp \rightarrow W^-Z+\text{jet}+X$:

PRELIMINARY!

LO versus NLO cross section at the LHC ($\mu = \mu_{\text{fact}} = \mu_{\text{ren}}$):



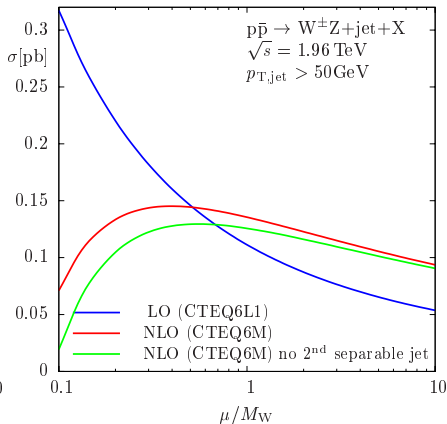
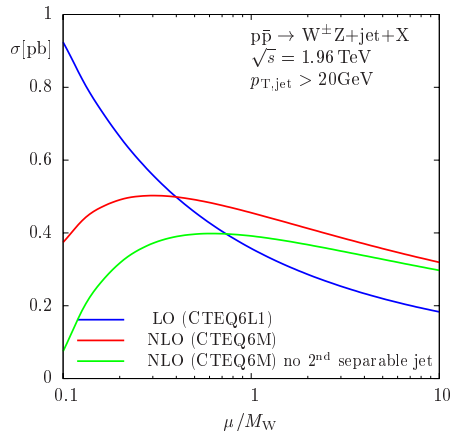
- Scale dependence stabilizes at NLO for genuine $W^-Z+\text{jet}$ production.
- But: Significant scale dependence is introduced by $W^-Z+2\text{jets}$ events.

Preliminary numerical results

Similar calculation performed for $p\bar{p} \rightarrow W^\pm Z + \text{jet} + X$:

PRELIMINARY!

LO versus NLO cross section at the Tevatron ($\mu = \mu_{\text{fact}} = \mu_{\text{ren}}$):



↪ Scale dependence stabilizes at NLO.
(only small influence from $WZ+2\text{jets}$ production)

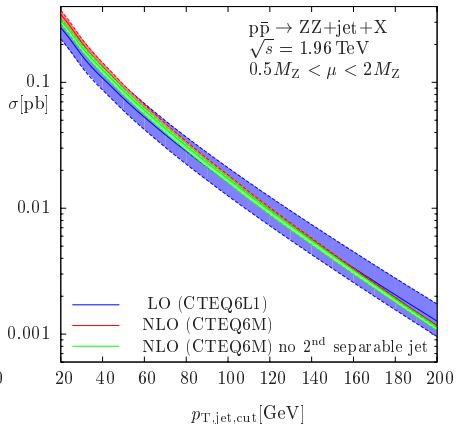
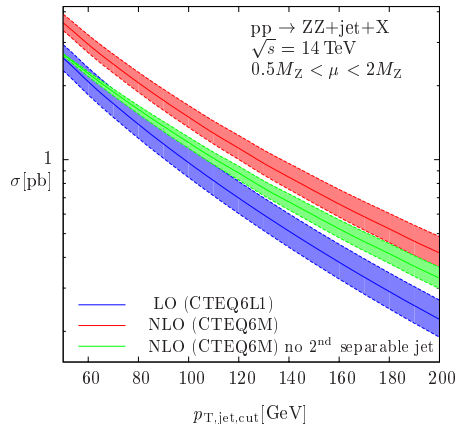
Preliminary numerical results

Similar calculation performed for $pp/p\bar{p} \rightarrow ZZ+\text{jet}+X$:

PRELIMINARY!

LO versus NLO cross section for $p_{T,\text{cut},\text{jet}}$ -variation at LHC and Tevatron:

($\mu = \mu_{\text{fact}} = \mu_{\text{ren}}$)



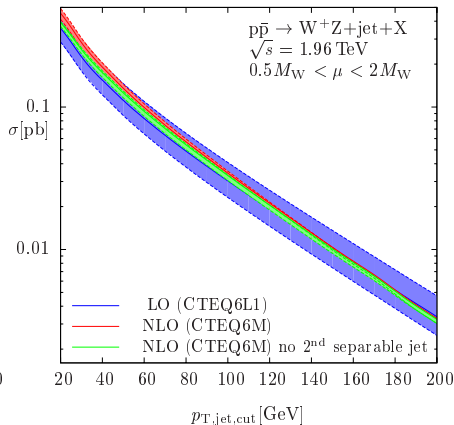
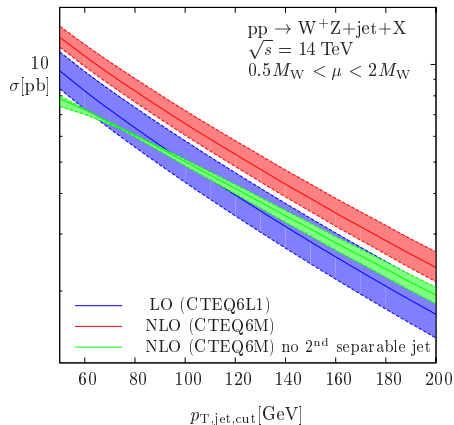
↪ Significant stabilisation of scale dependence is achieved at NLO
(at LHC especially for genuine ZZ+jet production)

Preliminary numerical results

Similar calculation performed for $pp/p\bar{p} \rightarrow W^+Z+\text{jet}+X$:

PRELIMINARY!

LO versus NLO cross section for $p_{T,\text{cut},\text{jet}}$ -variation at LHC and Tevatron:
($\mu = \mu_{\text{fact}} = \mu_{\text{ren}}$)



↪ Significant stabilisation of scale dependence is achieved at NLO
(at LHC especially for genuine $W^+Z+\text{jet}$ production)

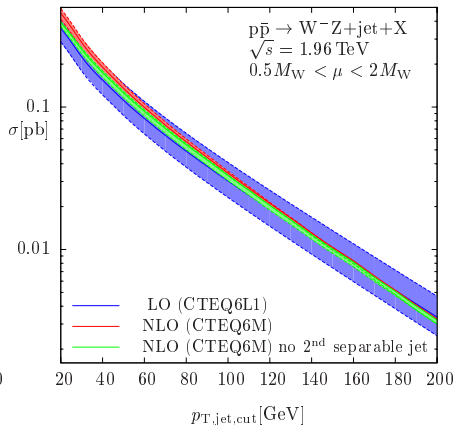
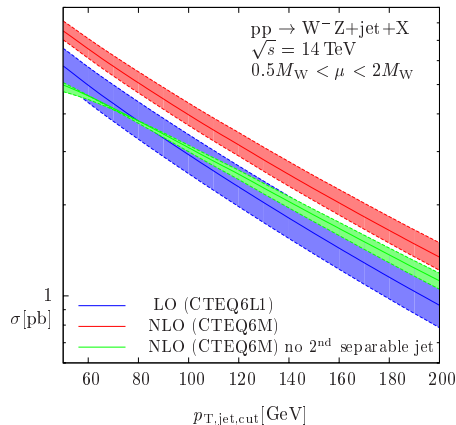
Preliminary numerical results

Similar calculation performed for $pp/p\bar{p} \rightarrow W^-Z+\text{jet}+X$:

PRELIMINARY!

LO versus NLO cross section for $p_{T,\text{cut},\text{jet}}$ -variation at LHC and Tevatron:

($\mu = \mu_{\text{fact}} = \mu_{\text{ren}}$)



↪ Significant stabilisation of scale dependence is achieved at NLO
(at LHC especially for genuine $W^-Z+\text{jet}$ production)